Review of Progress in Optical Ring Resonators with Crosstalk Modelling in OADMS

Riyadh Mansoor, and Alistair Duffy
School of Engineering and Sustainable Developments, DMU
Leicester, UK
riyadh.mansoor@email.dmu.ac.uk, apd@dmu.ac.uk

Abstract
In this paper, an overview of the optical ring resonators operation principle, fabrication and applications is presented. Emphasis was given for their add/drop functionality in Wavelength Division Multiplexing (WDM) networks. Ring resonator based Optical Add/Drop Multiplexer (OADMs) and filters are shown to be good candidates to realize Planar Lightwave Circuits (PLCs). They have a small 'real estate' requirement and are therefore potentially useful for large scale integrated optical circuits. However, like any other optical filters, ring resonator based OADMs are prone to crosstalk. The crosstalk suppression ratio (which is defined as the difference between the drop and through port responses at resonance) is shown to be highly affected by coupling coefficients. Controlling the coupling coefficients through careful design of the waveguide cross section, separation gap, and the length of the coupling region allows for increased crosstalk suppression ratio. Crosstalk in ring resonator based OADMs is modelled in this paper and an overview of the current state of knowledge about mitigating crosstalk is presented.

Keywords: Add/drop multiplexer, Bit error rate, Crosstalk, Ring resonators, Silicon-On-Insulator, sidewall roughness.

1. Introduction
Wavelength-Division-Multiplexing (WDM) using Silicon-On-Insulator (SOI) waveguides has become an attractive area of research to enable high integration density of photonic components as well as to ensure high speed data transmission [1]. In SOI technology, the high index contrast between core and cladding materials allows for light propagation in a small cross-section silicon waveguide with very little optical leakage [2]. Therefore, SOI is suitable for integrating photonic components at the micrometer scale [3].

WDM communication networks require optical components which can separate closely spaced channels effectively and allow for the flexible addition and dropping of channels [4]. Add/drop multiplexers (OADMs) and filters that drop one channel of WDM signal, without disturbing other channels, are essential elements in all-optical networks [5, 6]. Ring resonator based OADMs for WDM networks are considered as one example of SOI technology [3]. Ring resonators are promising devices for different applications in all-optical networks, such as filters, switches and optical delay lines [7-9]. Their small size allows for high density integration in optical photonic circuits by exploiting the availability of CMOS fabrication facilities [10]. Coupling a closed loop resonator with a bus waveguide leads to a new structure with a filter-like behaviour. Careful choice of the coupling coefficients between ring and bus waveguides has a great effect on the filter crosstalk performance.

This paper presents a review in the progress of optical ring resonators with the aim of modelling the crosstalk in OADMs. Inter and intra-band crosstalk in ring resonator OADMs is modelled, and the current state of knowledge for crosstalk mitigation techniques in WDM networks is presented.

2. Optical Ring Resonators
Ring resonators were first proposed by Marcatili [11] to support travelling wave resonant modes. A re-entrant waveguide with a perimeter of several μm was used to construct an optical resonator. The resonator was coupled to an external waveguide to get a transfer of the optical energy. The resultant structure (shown in Figure 1) supports a number of circulating wavelengths that satisfy the resonance condition $m \cdot \lambda_{res} = n_{eff} \cdot l$, where, m is an integer represents the mode number, l is the average resonator perimeter, and n_{eff} is the effective refractive index. The difference between two consecutive resonances is called the Free Spectral Range (FSR), which is of great interest in WDM systems.

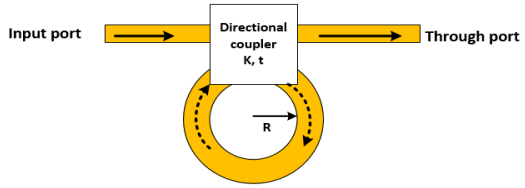

Figure 1. A schematic diagram of a ring resonator based all-pass filter.

If a WDM signal is launched at the input port in Figure 1, wavelengths that satisfy the resonant condition will be coupled to the ring. The constructive interference after each round trip results in an increase of the optical power in the resonator. The transfer of optical power is realized by exploiting the coupling between the evanescent modes in the ring and bus waveguide. This structure represents a ring resonator based all-pass filter which is used for dispersion compensation in WDM networks [12]. In the ring resonator based OADM (Figure 2) there is another bus waveguide coupled to the resonator. Therefore, the stored energy will coupled to the output waveguide leading to a build-up of optical power at the drop port and resulting in a notch in the through port response (due to coupling) [13, 14]. The resonator length and refractive index contrast determine the resonant wavelength, whereas, the coupling and loss coefficients are responsible for deciding the spectral response shape. Coupling coefficients are dependent on the coupling region characteristics (separation gap and coupling length), while losses are related to the type of materials used and the length of resonator, as well [15].

The propagation of light in any bounded medium is based on the refractive index contrast [16]. Low index contrast (LIC) materials were used first for optical waveguide fabrication, where the difference between core and cladding refractive indices is low. A reduction of the propagation loss was achieved using conventional LIC devices [17]. However, large radius resonators were required to ensure high confinement of the light. This means large size

components with a small FSR (FSR is inversely related to the radius).

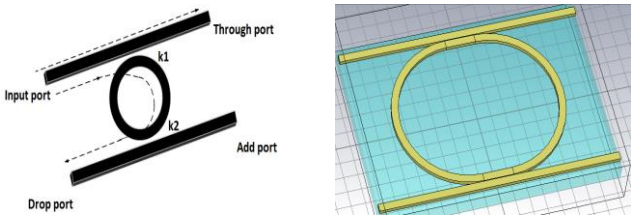

a b

Figure 2. a. Ring resonator add/drop filter. b. Racetrack resonator based OADM.

The FSR is required to be as high as possible to accommodate a wide bandwidth in the C-window (1535-1565 nm). Therefore, a number of rings (with different radii) were coupled in series to increase the FSR using the Vernier effect [18-20]. The Vernier effect extends the FSR by reducing all resonances which are not an integer multiple of the FSR of each individual ring. The new FSR is related to the FSR of each ring as [21]:

$$FSR_{extended} = n_1 FSR_1 = n_2 FSR_2$$

Where, n_1 and n_2 are integers.

Figure 3 shows how the Vernier effect is used to increase the FSR. For example, to obtain a 4.8 THz Free Spectral Range (wider than the C-window), a small ring with 2.23 µm radius is required (dotted red line in Figure 3). Using such small ring radius will increase bending loss and complexity. Therefore, two rings of 9 µm and 11.1 µm can be coupled in series to obtain similar FSR (blue line in Figure 3). This will reduce the complexity and losses.

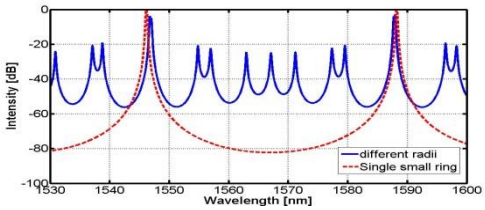

Figure 3. Analytically calculated drop port response of a series double RR with different radii (blue line) and identical radii (dotted red line).

The advancement in fabrication technologies has enabled the construction of small radii resonators using high index contrast material (HIC) [22]. High index contrast between core and cladding refractive indices results in a strong confinement of light even with a small bend radius. A large FSR (up to 32 nm) with a low level of bending loss has been achieved [3]. Polycrystalline silicon (poly Si) waveguides were proposed in [23] with radii of 3 ,4, and 5 µm and a FSR about 20-30 nm. The disadvantage of this design was the presence of a high insertion loss in the through port. Silicon nitride SiN was also used in [24] and a ring of radius 8 µm was fabricated to achieve 20 nm FSR. Recently, Silicon-On-Insulator (SOI) has been used which allows for the fabrication of small radius rings (using CMOS technology) with low bending and scattering losses [25].

Silicon-On-Insulator (SOI) waveguides are a promising technology for integrated photonic devices in WDM networks [26]. In this technology the propagation loss is relatively low [27]. However, the back reflection effect due to sidewall roughness is of great importance [28, 29]. Sidewall roughness is usually considered as a random perturbation and back reflection is treated as a stochastic variable [29].

The analytical calculations in [21] showed that the performance of a resonator is strongly affected by the characteristics of the surface roughness. The statistics of the sidewall roughness induced back reflection were investigated experimentally, first, in uncoupled optical waveguides [30]. It was shown that the intensity of back reflection follows the distribution of a single scattering system with a strong dependence upon waveguide length. Secondly, the change in back reflection characteristics when a ring resonator is coupled to an optical waveguide was examined in [31] and showed that, after a multiple round trip in the ring resonator, back reflection increases coherently and can affect the behaviour of the filter even at moderate quality factors (high coupling coefficients). In rough-walled ring resonators, back reflection is a well-known cause of resonance splitting due to mutual coupling between forward and counter-directional modes [21, 32-35]. This effect has been exploited to improve the extinction ratio by increasing the depth of the through port at resonance [32].

SOI ring resonators are receiving an increased level of attention from many research groups. IMEC (Belgium) is one of the centres that work on the use of SOI single mode optical waveguides [34, 36]. They fabricated a ring resonator with a 5 µm radius [37]with losses ranging from 2.5-3 dB/cm and FSR of 13.7 nm. Other groups such as the Institute fur Halbeitertechni (Germany) [1, 38], California Institute of Technology [39], the University of Wisconsin-Madison (USA) [40], and the Politecnico di Milano (Italy) [31, 35, 41], have fabricated ring and race track SOI resonators for different applications. Reducing the ring size leads to an increase in the coupling coefficient sensitivity to fabrication process (due to close proximity between ring and bus waveguides). To reduce the coupling coefficient sensitivity, a straight waveguide section was introduced to increase the coupling region. The resulting shape is a racetrack-like resonator (Figure 2 b) [42]. However, this will increase the resonator perimeter and results in a reduced FSR. Racetrack resonators with improved FSR were designed using the Vernier effect [43, 44].

Ring resonators can be used to drop single or multiple channels from WDM signal [45, 46]. A four channel dropping structure was proposed based on a compact parent-sub micro-ring resonator [43]. Also, nine channel OADM was fabricated by using SOI resonators [47]. Series and parallel coupled ring resonators have been proposed and used to enhance the spectral characteristics of OADMs by increasing the out of band rejection ratio and obtaining a sharp roll-off from pass-band to stop-band [48-52].

3. Coupling in Ring Resonators

There are two main approaches in which the coupling of light between the bent and bus waveguides is achieved: lateral and vertical coupling. The waveguide cross section in each scheme is different in order to support the required mode for each case. The TE mode is the dominant mode for the lateral coupling. For vertical coupling, the TM mode is dominant.

3.1. Lateral Coupling

If the bus and bent waveguides are placed in the same plane, as shown in Figure 4, the coupling will take place horizontally. This is the lateral coupling configuration. The coupling strength is controlled by the gap width between waveguides. The small gap

size required to ensure strong coupling in a HIC material makes this scheme of high sensitivity to the engraving and lithography procedures [53].

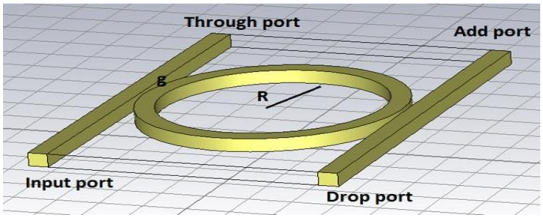

Figure 4. Laterally coupled ring resonator.

3.2. Vertical Coupling

In a vertical coupling configuration, bus and bent waveguides are etched in different layers (as shown in Figure 5). From the design point of view, this means increased flexibility because the ring and bus waveguides can be optimized separately [54]. The separation layer thickness (d) and the lateral deviation between bus waveguides and the ring will affect the coupling strength in this scheme [55]. Enhancing the crosstalk performance of a vertical coupled OADM, by optimizing the ring parameters.

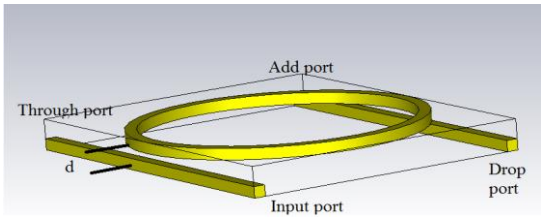

Figure 5. Vertical coupled ring resonator.

4. Cascaded Coupled Ring Resonators.

OADM improved spectral characteristics such as flat pass band response, high out-of-band rejection ratio and sharp step function can be obtained by using multiple (series or parallel) coupled ring resonators.

4.1. Series Coupling

Figure 6 shows the schematic of series coupled double ring resonators. Several rings can be placed between the input and the output bus waveguides. The outer coupling coefficients (between bus waveguides and outer rings) and the coupling between inter-rings are modelled by directional couplers with coupling coefficients, k_n, and through coupling coefficient t_n. If a defined WDM signal is injected as a source at the input port (port 1 in Figure 6), the frequency response will be as follows:

1. Off-resonance, the fraction of light, which has completed a single round trip in the first ring, interferes destructively with the light that has just coupled to the ring. There will be no build-up of the power inside the resonator. Only a small amount of light will couple to the second ring. The light remains mainly in the bus waveguides and propagates to the through port.
2. At resonance, the fraction of light that has just completed one round-trip in the first ring interferes constructively with the light coupled to the ring resulting in a coherent build-up of the power inside the ring resonator. After multiple coupling between inner-rings, the light will be dropped at port 3 (Figure 6) if the number of rings is odd, or it will be dropped at port 4 (opposite to port 3) if the number of rings is even.

Ring radii are either of the same size to support similar resonance wavelengths or with different sizes arranged to support a specific wavelength based on the Vernier effect [43, 44].

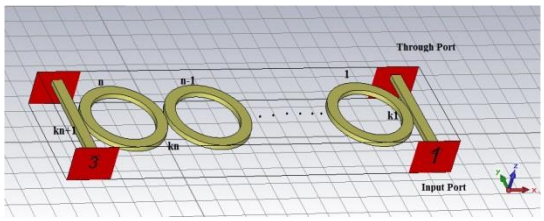

Figure 6. The schematic of N-series coupled ring resonator.

4.2. Parallel Coupling

In this configuration, rings are arranged in such a way that there is no direct coupling between the nearest neighbouring rings (as shown in Figure 7). Therefore, it offers more flexibility in the fabrication process compared to the serial configuration (no inter-ring coupling). The centre-to-centre separation between the nearest neighbour rings (L_r) will determine the filter response. Therefore, this distance should be chosen carefully to obtain the desired interference at the specified wavelength range. The useful wavelength range is rather limited due to the phase change that occurs due to the separation (L_r) between the rings. Outside this range the output of the drop port will vary in an undesirable way due to the interference of light coming from the individual resonators.

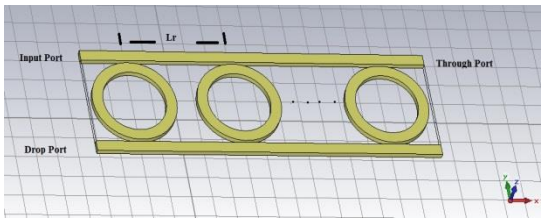

Figure 7. The schematic of N-parallel coupled ring resonator.

5. Ring Resonator Based OADMs

In this configuration, two directional couplers are formed as shown in Figure 8. Directional couplers are defined by coupling coefficient (k), and through coefficient (t) [56]. The coupling region length, gap width and refractive index profile determine the values of k^2 and t^2. For lossless coupling, $k^2 + t^2 = 1$. However, the coupling losses are included in the loss coefficient α of the ring which determines the total reduction of the wave after one round trip.

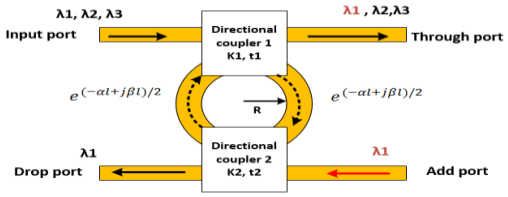

Figure 8. Schematic diagram of the ring resonator based OADM.

The spectral responses of ring resonator based OADMs are highly affected by the coupling region's characteristics. Symmetrical coupled OADMs are realized by similar directional couplers (i.e $k_1 = k_2$). OADMs are said to be asymmetrically coupled if

$k_1 \neq k_2$, which is physically realized by a different separation gap in each side of the ring [52, 57]. The drop and through port transfer functions of a single ring resonator OADM are calculated using the space domain Coupled Mode Theory (CMT) [10, 15, 58], as in (1) and (2), respectively:

$$G_d = \frac{-k_1 k_2 \cdot x^{1/2}}{1 - t_1 t_2 x} \quad (1)$$

$$G_{th} = \frac{(t_1 - t_2 x)}{1 - t_1 t_2 x} \quad (2)$$

Where, $x = e^{(-\alpha l - j\beta l)}$ is the round trip propagation coefficient and l is the ring perimeter. Coupling and loss coefficients affect all the filter parameters, starting from the insertion loss to finesse as shown in equations (3) to (10) below:

1. Through port response (Insertion loss):

$$IR = |G_{th}|^2 = \frac{{t_2}^2 e^{-2\alpha l} - 2t_1 t_2 e^{-\alpha l}\cos\beta l + {t_1}^2}{1 - 2t_1 t_2 e^{-\alpha l}\cos\beta l + {t_1}^2 {t_2}^2 e^{-2\alpha l}} \quad (3)$$

At resonance (through port notch):

$$IR_{res} = \frac{\left(t_2 e^{-\alpha l} - t_1\right)^2}{(1 - t_1 t_2 e^{-\alpha l})^2} \quad (4)$$

The ratio between the maximum and minimum values of the through port response represents the extinction ratio, ER_{th}:

$$ER_{th} = \frac{IR_{max}}{IR_{res}} = \left[\frac{\left(1 - t_1 t_2 e^{-\alpha l}\right) \cdot \left(t_2 e^{-\alpha l} + t_1\right)}{\left(t_2 e^{-\alpha l} - t_1\right) \cdot \left(1 + t_1 t_2 e^{-\alpha l}\right)}\right]^2$$

2. Drop port response:

$$DR = |G_d|^2 = \frac{{k_1}^2 {k_2}^2 e^{-\alpha l}}{1 - 2t_1 t_2 e^{-\alpha l}\cos\beta l + {t_1}^2 {t_2}^2 e^{-2\alpha l}} \quad (5)$$

At resonance:

$$DR_{res} = \frac{{k_1}^2 {k_2}^2 e^{-\alpha l}}{(1 - t_1 t_2 e^{-\alpha l})^2} \quad (6)$$

The ratio between the maximum and minimum values of the drop port response represents the out-of-band rejection ratio, OBRR:

$$OBRR = \frac{(1 + t_1 t_2 e^{-\alpha l})^2}{(1 - t_1 t_2 e^{-\alpha l})^2}$$

3. Free spectral range (FSR): the frequency separation between two consecutive resonances [34].

$$FSR = \lambda_{res+1} - \lambda_{res} \cong \frac{{\lambda_{res}}^2}{n_g l} \quad (7)$$

4. Full width at half maximum FWHM:

$$FWHM = \frac{(1 - t_1 t_2 e^{-\alpha l}) \cdot {\lambda_{res}}^2}{\pi n_g l \cdot \sqrt{t_1 t_2 e^{-\alpha l}}} \quad (8)$$

5. Q-factor, measures the number of round trips of the stored energy before it drops to 0.367 (=1/e) of its initial value, mathematically it can be expressed as:

$$Q_{factor} = \frac{\lambda_{res}}{FWHM} = \frac{\pi n_g l \cdot \sqrt{t_1 t_2 \cdot e^{-\alpha l}}}{\lambda_{res} \cdot (1 - t_1 t_2 \cdot e^{-\alpha l})} \quad (9)$$

6. Finesse: is a measure of the ratio between the resonances' sharpness to their spacing, mathematically, it can be expressed as [34]:

$$Finesse = \frac{FSR}{FWHM} = \frac{\pi \cdot \sqrt{t_1 t_2 \cdot e^{-\alpha l}}}{(1 - t_1 t_2 \cdot e^{-\alpha l})} \quad (10)$$

7. Crosstalk suppression: is defined as the difference between the drop and through port intensities at the resonance. It represents the level of suppression of the unwanted channels; mathematically it can be expressed as the difference between equations (9) and (6).
8. Losses: the losses can be caused due to different factors such as coupling losses and round trip losses (propagation losses, sidewall roughness and fabrication mismatch of waveguide width). All the losses are included in the attenuation term (α), and used in all equation as $e^{-\alpha \cdot l}$.

The key factors to assess the OADM performance are the through port notch depth, maximum power dropped and the crosstalk suppression ratio at resonance. Equations (3) to (10) show that a careful choice of the coupling coefficient will result in substantial performance enhancement. A typical frequency response of a single ring resonator OADM is presented in Figure 9. It was calculated using CST [59]. The through and drop port responses are shown in this figure. Free spectral range (FSR) also explained and Out of Band Rejection Ratio (OBRR) are illustrated in this diagram.

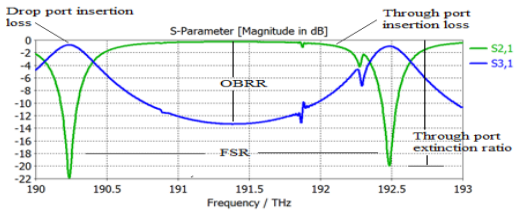

Figure 9. CST simulated frequency response of a single ring resonator based OADM.

6. Crosstalk Modelling in Ring Resonators Based OADMs

Crosstalk in ring resonator based OADMs results from the non-ideal dropping of channels [49]. The dropped channel will be corrupted by the residual of the new added channel (intra-band crosstalk). Inter-band crosstalk also occurs due to the adjacent channels in a WDM signal [60]. In this section, the optical system that uses on/off keying transmission is studied for crosstalk modelling, without loss of generality [61]. The optical field can be considered as a continuous wave CW of the form:

$$\mathbf{E_s(t)} = \hat{r}_s \sqrt{P_s(t)} \cdot e^{(j\omega_s t + j\emptyset_s(t))} \quad (11)$$

Where (P_s) the optical power, $\hat{r}_s$ represents the state of polarization, ω_s is the frequency of light, and $\emptyset_s(t)$ is the instantaneous optical phase.

After the propagation of the optical signal in an all-optical network, many crosstalk terms will disturb it. The corrupted optical field at the receiver input will be a combination of the desired signal and the intra-system noise, and can be expressed as:

$$\mathbf{E_{ph}(t)} = \mathbf{E_s(t)} + \sum_k \mathbf{E_k(t)}$$

$$= \hat{r}_s\sqrt{P_s}\cdot b_s(t)e^{(j\omega_s t+j\emptyset_s(t))} + \sum_{k=2}^{N}\hat{r}_k\sqrt{\epsilon_k P_s} \cdot b_k(t)e^{(j\omega_k t+j\emptyset_k(t))} \quad (12)$$

Where, $\epsilon_k = \frac{P_k}{P_s}$ is the power ratio of the k_{th} crosstalk component to the dropped channel power. $b_s(t)$ and $b_k(t)$ represent the binary symbols forming the amplitude modulating signal $\in\{0,1\}$.

The receiver in such systems consists of a photo-detector followed by an electrical filter and a decision (threshold) circuit [62, 63]. The photo-detector output current is proportional to the square of the incident optical field. The output of an electrical filter is, then compared with a decision threshold level (I_D) to decide whether a "1" or "0" state was sent. The power leakage from unwanted channels may lead to a "1" state at the receiver side while the transmitted signal is "0" or vice versa, this will reduce the system performance and increase the bit error rate (BER).

The receiver photo-current can be written as:

$$i_{ph}(t) = \rho\left|E_{ph}(t)\right|^2 = \rho\left|E_s(t) + \sum_k E_k(t)\right|^2 \quad (13)$$

Where ρ represent the photodiode responsitivity and it will be considered equal to unity for simplicity. The general form of the photo current will consists of four terms [62] as below:

1. The signal power $[P_s b_s(t)]$.
2. The crosstalk power $[P_s \sum_{k=2}^{N} b_k(t)\,\epsilon_k]$.
3. The channel-crosstalk beating term

$$[2P_s \cdot \sum_{k=2}^{N}\hat{r}_s\cdot\hat{r}_k\sqrt{\epsilon_k}\cdot b_k(t)b_s(t) \cdot \cos[(\omega_s-\omega_k)t+\emptyset_s(t)-\emptyset_k(t)]]$$

4. The crosstalk-crosstalk beat noise, which is of less importance in the study of the system performance in terms of crosstalk impairment [64].

$$[2P_s \cdot \sum_{k=2}^{N-1}\sum_{l=k+1}^{N}\hat{r}_k\cdot\hat{r}_l\sqrt{\epsilon_k\epsilon_l}\cdot b_k(t)b_l(t) \cdot \cos[(\omega_k-\omega_l)t+\emptyset_k(t)-\emptyset_l(t)]]$$

The total current can be written as in Equation (14) below:

$$i_{ph}(t) = P_s[b_s(t) + \sum_{k=2}^{N} b_k(t)\,\epsilon_k + 2\cdot\sum_{k=2}^{N}\hat{r}_s.\hat{r}_k\sqrt{\epsilon_k} \cdot b_k(t)b_s(t) \cdot \cos[(\omega_s-\omega_k)t+\emptyset_s(t)-\emptyset_k(t)] + 2\cdot\sum_{k=2}^{N-1}\sum_{l=k+1}^{N}\hat{r}_k\cdot\hat{r}_l\sqrt{\epsilon_k\epsilon_l} \cdot b_k(t)b_l(t) \cdot \cos[(\omega_k-\omega_l)t+\emptyset_k(t) - \emptyset_l(t)]] \quad (14)$$

The most important crosstalk contribution is the signal-crosstalk beating term which can be considered as a random variable in term of the phase [65].

6.1. Inter-Band Crosstalk

Considering the case that OADM is used to drop a single channel among N WDM channels at the input port. The dropped channel will be corrupted by the residual of (N-1) adjacent channels. The drop port photo-current will consist of two terms (as in (15)), $i_s$is the receiver current due to the dropped channel, and i_n is the summation of crosstalk currents resulting from the leaked power of (N-1) adjacent channels.

Based on equation (14):

$$i = i_s + i_n = P_s[b_s(t) + \sum_{k=2}^{N} b_k(t)\,\epsilon_k] \quad (15)$$

The third and fourth terms of equation (14) are small and neglected due to the frequency difference between the dropped and unwanted channels.

The level of crosstalk current i_n depends on:

1. The bit pattern of the (N-1) channels $b_k(t)$. i_n becomes maximum when all channels are in "1" state simultaneously, which represent the worst case.
2. The suppression ratio (ϵ_k) for each adjacent channel (drop port response).

Figure 10 shows the suppression ratio (ϵ_k) for three channels separated by 50 GHz (as specified by the ITU-T G.694.1 telecommunication standards [60]), in a single and double ring resonator based OADM. For a single ring OADM, based on the drop port response (solid line in Figure 10), the suppression ratio is:

1. For first adjacent channel (50 GHz from the resonance), ϵ_k=−5. dB.
2. For the second channel (100 GHz from the resonance), ϵ_k=−10. dB.
3. For the third channel (150 GHz from the resonance), ϵ_k=−12 dB.

However, the drop port response depends on the coupling coefficients and also on the number of resonators used (cascaded rings). Increasing the order of the filter (the number of rings) will lead to a sharp transition in the spectral response as shown in Figure 10 (dashed line). Hence, a reduction in the inter-band crosstalk can be achieved. The suppression ratio for adjacent channels in a double ring resonator OADM are: −14.5 dB, −26.5 dB and −32.7 dB for a 50 GHz, 100 GHz and 150 GHz spaced channels, respectively. Reducing the effect of inter-band crosstalk requires enhancing the drop port response shape by using multiple rings (increasing the order of the filter [66, 67].

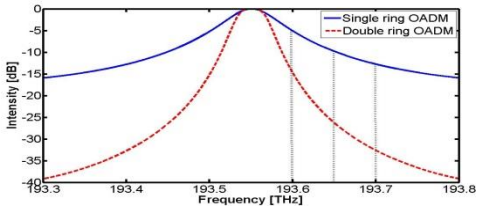

Figure 10. Drop port response for single (solid) and double (dashed) ring resonators.

6.2. Intra-Band Crosstalk

Intra-band crosstalk is the main source of system performance degradation in all-optical networks [5]. It occurs due to the power leakage from the new added channel $E_a(t)$ of a similar wavelength to that of the dropped channel $E_d(t)$.

The photo current at the receiver can be expressed as:

$$i_{ph}(t) = \rho\left|E_{ph}(t)\right|^2 = \rho|E_d(t) + E_a(t)|^2 \quad (16)$$

The photo-current in (14) can be re-written as in [68]:

$$i = [{P_d}^2 + {P_a}^2 + 2 \cdot \sqrt{P_d P_a} \cdot \cos(\phi_d(t) - \phi_a(t))] \quad (17)$$

Equation (17) consists of three terms:

1. The dropped channel photo-current.
2. The added channel photo-current, which is small due to suppression.
3. Crosstalk current resulting from the beating between $E_a(t)$ and $E_d(t)$. The worst case is studied where the crosstalk term and the dropped signal are in phase [16].

Following the calculations of [69], BER at the receiver is:

$$BER = \frac{1}{4} \cdot \text{erfc}\left(\frac{1}{\sqrt{2}} \cdot \frac{i - I_D}{\delta_1}\right) + \frac{1}{4} \cdot \text{erfc}\left(\frac{1}{\sqrt{2}} \cdot \frac{I_D}{\delta_0}\right) \quad (18)$$

1. The first term of this equation represents the BER for "1" state where the receiver's current is i, while the second term is for a "0" state.
2. I_D is the threshold level.
3. erfc represents the complementary error function [70].
4. δ_0 is the receiver noise which exists in the absence of crosstalk (it is mainly due to thermal noise) for the "0" state.
5. δ_1 represents the sum of the beating term of crosstalk and receiver noise ($\delta_1 = \sqrt{{\delta_0}^2 + \gamma \cdot i^2}$) for the "1" state [71].
6. $\gamma = \frac{P_a}{P_d}$ is the crosstalk suppression ratio as shown in Figure 11.

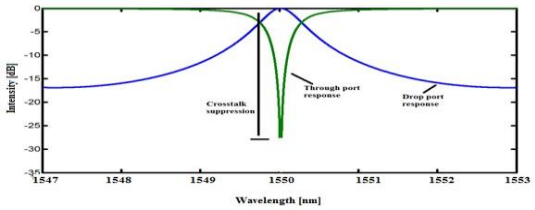

Figure 11. Power penalty as a function of crosstalk suppression ratio.

Using the optimum threshold value of I_D given by [69]:

$$I_D = \frac{i}{\delta_0 + \sqrt{{\delta_0}^2 + \gamma \cdot i^2}}$$

BER is:

$$BER = \frac{1}{2} \cdot \text{erfc}\left(\frac{1}{\sqrt{2}} \cdot Q\right)$$

Where, $Q = \frac{i}{\sqrt{\delta 0^2 + \gamma \cdot i^2}}$.

To evaluate the effect of intra-band crosstalk, the power penalty should be considered. Power penalty is defined as the amount of power to be added to overcome the effect of crosstalk and maintain same BER in the absence of crosstalk.

The power penalty (x) is [69]:

$$x = -10 \cdot \log[1 - \gamma \cdot Q^2] \quad (19)$$

For BER=10^{-9}, Q = 6 [72].

The power penalty required to counteract the intra-band crosstalk effect depends on γ (crosstalk suppression ratio) which is in ring resonators based OADM represents the difference between the drop and through port responses at resonance (Figure 11). Equation (19) is plotted in Figure 12 to show the relation between the crosstalk suppression ratio (α) and the required power penalty to obtain BER=10^{-9}.

In Figure 12, for a crosstalk suppression ratio being higher than |20| dB, a high reduction in the imposed power penalty can be achieved. Allowing for high values of crosstalk suppression ratios (at resonance) will reduce the required power penalty. However, for WDM networks, the crosstalk suppression should be kept high over the whole frequency range of modulated channels in order to ensure efficient dropping with low level of crosstalk.

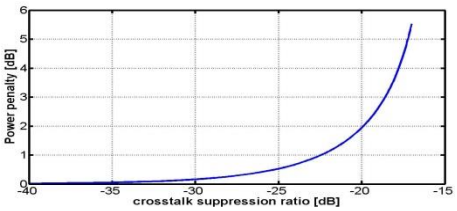

Figure 12. Power penalty as a function of crosstalk suppression ratio.

7. Mitigation of Crosstalk in Ring Resonators based OADMs

Crosstalk effect in ring resonators based OADMs was studied numerically in [5, 73]. Intra-band crosstalk effects were estimated by calculating the eye opening penalty at the receiver side. The drop port rejection ratio at the wavelength of the adjacent channel was used to estimate the inter-band crosstalk effect. A multi-stage topology was suggested in [5]to reduce the effect of crosstalk for different data rates. In this topology, the first stage is optimized for low crosstalk in the drop port channel, while another stage is used for the added channel crosstalk mitigation. However, this required an increase in the filter size. The use of an active ring was suggested in [73]to eliminate the intra-band crosstalk effect. Analytical calculations were performed to estimate the crosstalk. However, the amplified spontaneous emission (ASE) effect of the semiconductor optical amplifier was not considered. A double–stage topology was proposed. The effect of crosstalk in lossy ring resonator based OADM was studied in [74]. The range of coupling coefficients to reduce the intra-band crosstalk was studied analytically. Vertical coupling, for greater control of coupling coefficients, was proposed.

Series coupling between ring resonators was proposed to increase the filter order [75, 76]. Increasing the filter order leads to an improvement in the spectral response and allows high suppression of the adjacent channel crosstalk (inter-band crosstalk). However, the sub-micrometer gap between the rings (inter-rings coupling coefficient) has a great effect on the overall response. The inter-ring coupling effect was addressed either by selecting the optimum coupling or by proper physical arrangement of the rings. The optimum condition for coupling coefficients to improve the crosstalk suppression ratio (only) was proposed in [75]. A formula that calculates the optimum coupling coefficient of different order

filters was analytically derived. The optimum coupling coefficients for a second order series coupled ring resonator in the presence of losses was studied. The optimal arrangement for a high order series coupled ring resonator was suggested in [76]. The dependence of the filter response of four series-coupled rings with two different ring radii on the arrangement of ring radii was investigated. An analytical study to calculate the effect of using rings with different radii on the inter-band crosstalk and how these arrangements work with high bit rate signals was presented [76].

Parallel coupling between ring resonators was also proposed to mitigate the crosstalk [77, 78]. In this coupling configuration, the spectral response depends on the phase relationship between rings (the separation between rings). It was shown in [77] that a number of ring resonators in parallel coupled configurations provide an improvement in the filter performance and reduces the inter-band crosstalk. Most attention was given to the out of band rejection ratio and how to reduce the inter-band crosstalk by controlling the separation between rings. In [78], the phase relationship between rings that affects the spectral response of the filter was studied experimentally. A box-like response was achieved, and high out of band rejection ration was obtained. However, filter size was increased. A cross-grid architecture (using a vertical coupled ring resonator) was proposed to increase the scalability. Cross-grid technology for crosstalk reduction was examined experimentally by [79]. The drawback of this technology is the intersection between optical waveguides that can lead to further crosstalk.

A “Racetrack” model of the resonator was used in [80] to increase the through port notch and improve the drop port response by using asymmetric coupling. In a racetrack resonator based OADM, the coupling region length is longer than that of ring resonator. This permits better control of the spectral response. An increase in the crosstalk suppression ratio was obtained. Increasing the filter order and also using a multi-stage structure was proposed in [24], but at the expense of filter size.

Most of the work to mitigate the crosstalk in ring resonator based OADMs was focused on either improving the filter response by increasing the filter order, or increasing the notch depth of the through port response (increasing the crosstalk suppression ratio). Increasing the filter order (the number of rings) or connecting different OADMs, giving a multi-stage structure, results in a reduction in the inter-band crosstalk. However, filter size will increase, conflicting with the goal of greater device density. Increasing the notch depth (by optimizing coupling coefficients) will only increase the crosstalk suppression ratio in a narrow band of frequencies at resonance. For modulated channels this implies that the side-bands will get different levels of suppression from that of the centre frequency. For example, for 10 Gbps non return-to-zero (NRZ) transmission, the required bandwidth is 20 GHz [6]. Therefore, having a high level of crosstalk suppression ratio for a bandwidth less than 20 GHz will still result in crosstalk. For a similar data rate with a return-to-zero (RZ) transmission, the bandwidth is 40 GHz.

Improving signal integrity in ring resonator OADMs for WDM applications was addressed by increasing the crosstalk suppression bandwidth rather than increasing the crosstalk suppression ratio. Crosstalk suppression bandwidth is defined as the bandwidth over which the crosstalk suppression ratio is maintained over an adequate level for a wide frequency range. Maintaining a high level of crosstalk suppression over a 20 GHz allows dropping 10 GBps NRZ signal with mitigated level of crosstalk. Improving the crosstalk suppression was achieved by controlling inter-ring coupling coefficient in series coupled ring resonator [81], optimizing coupling coefficients in vertically coupled ring resonator [55] and exploiting controllable reflectivity in rough-walled ring resonators [82].

8. Conclusions

This paper has presented an overview of the progress in optical ring resonators with more emphasis in their add/drop functionality in WDM networks. Basic structures (lateral and vertical coupling) of ring resonator OADM, as well as cascaded coupled ring resonators OADM were discussed. General equations that represent different port responses were presented. Inter and intra-band crosstalk in OADMs were modelled and the different approaches for crosstalk mitigation are reviewed. Optical ring resonator based filters and multiplexers are ubiquitous components in all optical networks. Therefore, mitigating the crosstalk in OADMs will allow for optical integrated circuits with high integration density and improved signal integrity.

9. References

[1] A. Vorckel, M. Monster, W. Henschel, P. H. Bolivar and H. Kurz, "Asymmetrically coupled silicon-on-insulator microring resonators for compact add-drop multiplexers," *Photonics Technology Letters, IEEE,* vol. 15, pp. 921-923, 2003.

[2] W. Bogaerts, M. Fiers and P. Dumon, "Design challenges in silicon photonics," *Selected Topics in Quantum Electronics, IEEE Journal Of,* vol. 20, pp. 1-8, 2014.

[3] S. Xiao, M. H. Khan, H. Shen and M. Qi, "Silicon-on-insulator microring add-drop filters with free spectral ranges over 30 nm," *J. Lightwave Technol.,* vol. 26, pp. 228-236, 2008.

[4] F. Xia, L. Sekaric and Y. A. Vlasov, "Mode conversion losses in silicon-on-insulator photonic wire based racetrack resonators," *Optics Express,* vol. 14, pp. 3872-3886, 2006.

[5] H. Simos, C. Mesaritakis, D. Alexandropoulos and D. Syvridis, "Dynamic analysis of crosstalk performance in microring-based add/drop filters," *J. Lightwave Technol.,* vol. 27, pp. 2027-2034, 2009.

[6] B. E. Little, S. T. Chu, H. A. Haus, J. Foresi and J. -. Laine, "Microring resonator channel dropping filters," *Lightwave Technology, Journal Of,* vol. 15, pp. 998-1005, 1997.

[7] D. G. Rabus, M. Hamacher, U. Troppenz and H. Heidrich, "High-Q channel-dropping filters using ring resonators with integrated SOAs," *Photonics Technology Letters, IEEE,* vol. 14, pp. 1442-1444, 2002.

[8] B. Little, S. Chu, P. Absil, J. Hryniewicz, F. Johnson, F. Seiferth, D. Gill, V. Van, O. King and M. Trakalo, "Very high-order microring resonator filters for WDM applications," *Photonics Technology Letters, IEEE,* vol. 16, pp. 2263-2265, 2004.

[9] A. Densmore, D. Xu, P. Waldron, S. Janz, P. Cheben, J. Lapointe, A. Delâge, B. Lamontagne, J. Schmid and E. Post, "A silicon-on-insulator photonic wire based evanescent field sensor," *Photonics Technology Letters, IEEE,* vol. 18, pp. 2520-2522, 2006.

[10] R. D. Mansoor, H. Sasse and A. P. Duffy, "Analysis of optical ring resonator add/drop filters," in *The 62nd IWCS,* USA, 2013, pp. 471-475.

[11] E. Marcatili, "Bends in optical dielectric guides," *Bell System Technical Journal,* vol. 48, pp. 2103-2132, 1969.

[12] C. Madsen and G. Lenz, "Optical all-pass filters for phase response design with applications for dispersion compensation," *Photonics Technology Letters, IEEE,* vol. 10, pp. 994-996, 1998.

[13] E. J. Klein, *Densely Integrated Microrooring-Resonator Based Components for Fiber-to-the-Home Applications.* University of Twente, 2007, http://purl.utwente.nl/publications/60711.

[14] C. Manolatou, M. Khan, S. Fan, P. R. Villeneuve, H. Haus and J. Joannopoulos, "Coupling of modes analysis of resonant channel add-drop filters," *Quantum Electronics, IEEE Journal Of,* vol. 35, pp. 1322-1331, 1999.

[15] A. Yariv, "Coupled-mode theory for guided-wave optics," *Quantum Electronics, IEEE Journal Of,* vol. 9, pp. 919-933, 1973.

[16] G. P. Agrawal, *Fiber-Optic Communication Systems.* New York, NY: John Wiley & Sons, 1997.

[17] A. Taflove, and S. C. Hagness, *Computational Electrodynamics: The Finite-Difference Time-Domain Method.* London: Artech House Inc., 3rd ed., 2005.

[18] C. Chaichuay, P. P. Yupapin and P. Saeung, "The serially coupled multiple ring resonator filters and Vernier effect," *Optica Applicata,* vol. 39, pp. 175-194, 2009.

[19] P. Urquhart, "Compound optical-fiber-based resonators," *JOSA A,* vol. 5, pp. 803-812, 1988.

[20] K. Oda, N. Takato and H. Toba, "A wide-FSR waveguide double-ring resonator for optical FDM transmission systems," *Lightwave Technology, Journal Of,* vol. 9, pp. 728-736, 1991.

[21] O. Schwelb, "The nature of spurious mode suppression in extended FSR microring multiplexers," *Opt. Commun.,* vol. 271, pp. 424-429, 2007.

[22] T. Barwicz, M. A. Popović, M. R. Watts, P. T. Rakich, E. P. Ippen and H. I. Smith, "Fabrication of add-drop filters based on frequency-matched microring resonators," *J. Lightwave Technol.,* vol. 24, pp. 2207, 2006.

[23] B. E. Little, J. Foresi, G. Steinmeyer, E. Thoen, S. Chu, H. Haus, E. Ippen, L. Kimerling and W. Greene, "Ultra-compact Si-SiO 2 microring resonator optical channel dropping filters," *Photonics Technology Letters, IEEE,* vol. 10, pp. 549-551, 1998.

[24] T. Barwicz, H. Byun, F. Gan, C. Holzwarth, M. Popovic, P. Rakich, M. Watts, E. Ippen, F. Kärtner and H. Smith, "Silicon photonics for compact, energy-efficient interconnects [Invited]," *Journal of Optical Networking,* vol. 6, pp. 63-73, 2007.

[25] O. Schwelb, "Microring resonator based photonic circuits: Analysis and design," in *Telecommunications in Modern Satellite, Cable and Broadcasting Services,* 2007, pp. 187-194.

[26] A. Bianco, D. Cuda, M. Garrich, G. G. Castillo, V. Martina and F. Neri, "Crosstalk minimization in microring-based wavelength routing matrices," in *Global Telecommunications Conference (GLOBECOM), IEEE,* 2011, pp. 1-5.

[27] G. Ballesteros, J. Matres, J. Martí and C. Oton, "Characterizing and modeling backscattering in silicon microring resonators," *Optics Express,* vol. 19, pp. 24980-24985, 2011.

[28] C. Sui, Q. Wang, S. Xiao and P. Li, "Analysis of Microdisk/Microring's Surface Roughness Effect by Orthogonal Decomposition," *Optics and Photonics Journal,* vol. 3, pp. 288, 2013.

[29] B. E. Little, J. Laine and S. T. Chu, "Surface-roughness-induced contradirectional coupling in ring and disk resonators," *Opt. Lett.,* vol. 22, pp. 4-6, 1997.

[30] F. Morichetti, A. Canciamilla and A. Melloni, "Statistics of backscattering in optical waveguides," *Opt. Lett.,* vol. 35, pp. 1777-1779, 2010.

[31] F. Morichetti, A. Canciamilla, M. Martinelli, A. Samarelli, R. De La Rue, M. Sorel and A. Melloni, "Coherent backscattering in optical microring resonators," *Appl. Phys. Lett.,* vol. 96, pp. 081112-081112-3, 2010.

[32] Z. Zhang, M. Dainese, L. Wosinski and M. Qiu, "Resonance-splitting and enhanced notch depth in SOI ring resonators with mutual mode coupling," *Optics Express,* vol. 16, pp. 4621-4630, 2008.

[33] G. T. Paloczi, J. Scheuer and A. Yariv, "Compact microring-based wavelength-selective inline optical reflector," *IEEE Photonics Technology Letters,* vol. 17, pp. 390-392, 2005.

[34] W. Bogaerts, P. De Heyn, T. Van Vaerenbergh, K. De Vos, S. Kumar Selvaraja, T. Claes, P. Dumon, P. Bienstman, D. Van Thourhout and R. Baets, "Silicon microring resonators," *Laser & Photonics Reviews,* vol. 6, pp. 47-73, 2012.

[35] C. Alonso-Ramos, F. Morichetti, A. Ortega-Monux, I. Molina-Fernandez, M. J. Strain and A. Melloni, "Dual-mode coupled-resonator integrated optical filters," *IEEE Photonics Technology Letters,* vol. 26, pp. 929-932, 2014.

[36] W. Bogaerts, R. Baets, P. Dumon, V. Wiaux, S. Beckx, D. Taillaert, B. Luyssaert, J. Van Campenhout, P. Bienstman and D. Van Thourhout, "Nanophotonic waveguides in silicon-on-insulator fabricated with CMOS technology," *Lightwave Technology, Journal Of,* vol. 23, pp. 401-412, 2005.

[37] P. Dumon, W. Bogaerts, V. Wiaux, J. Wouters, S. Beckx, J. Van Campenhout, D. Taillaert, B. Luyssaert, P. Bienstman and D. Van Thourhout, "Low-loss SOI photonic wires and ring resonators fabricated with deep UV lithography," *IEEE Photonics Technology Letters,* vol. 16, pp. 1328-1330, 2004.

[38] J. Niehusmann, A. Vörckel, P. H. Bolivar, T. Wahlbrink, W. Henschel and H. Kurz, "Ultrahigh-quality-factor silicon-on-insulator microring resonator," *Opt. Lett.,* vol. 29, pp. 2861-2863, 2004.

[39] T. Baehr-Jones, M. Hochberg, C. Walker and A. Scherer, "High-Q ring resonators in thin silicon-on-insulator," *Appl. Phys. Lett.,* vol. 85, pp. 3346-3347, 2004.

[40] X. Zhang and X. Li, "Design, fabrication and characterization of optical microring sensors on metal substrates," *J Micromech Microengineering,* vol. 18, pp. 015025, 2008.

[41] A. Parini, G. Bellanca, A. Annoni, F. Morichetti, A. Melloni, M. Strain, M. Sorel, M. Gay, C. Pareige and L. Bramerie, "BER Evaluation of a Passive SOI WDM Router," *IEEE Photonics Technology Letters,* vol. 25, pp. 2285-2288, 2013.

[42] R. Grover, T. Ibrahim, T. Ding, Y. Leng, L. Kuo, S. Kanakaraju, K. Amarnath, L. Calhoun and P. Ho, "Laterally coupled InP-based single-mode microracetrack notch filter," *Photonics Technology Letters, IEEE,* vol. 15, pp. 1082-1084, 2003.

[43] H. Yan, X. Feng, D. Zhang and Y. Huang, "Integrated optical add-drop multiplexer based on a compact parent-sub microring-resonator structure," *Opt. Commun.*, vol. 289, pp. 53-59, 2012.

[44] R. Boeck, N. A. Jaeger, N. Rouger and L. Chrostowski, "Series-coupled silicon racetrack resonators and the Vernier effect: theory and measurement," *Optics Express*, vol. 18, pp. 25151-25157, 2010.

[45] R. Orta, P. Savi, R. Tascone and D. Trinchero, "Synthesis of multiple-ring-resonator filters for optical systems," *Photonics Technology Letters, IEEE*, vol. 7, pp. 1447-1449, 1995.

[46] A. Melloni and M. Martinelli, "Synthesis of direct-coupled-resonators bandpass filters for WDM systems," *Lightwave Technology, Journal Of*, vol. 20, pp. 296-303, 2002.

[47] S. Xiao, M. H. Khan, H. Shen and M. Qi, "Multiple-channel silicon micro-resonator based filters for WDM applications," *Optics Express*, vol. 15, pp. 7489-7498, 2007.

[48] M. S. Dahlem, C. W. Holzwarth, A. Khilo, F. X. Kärtner, H. I. Smith and E. P. Ippen, "Eleven-channel second-order silicon microring-resonator filterbank with tunable channel spacing," in *Conference on Lasers and Electro-Optics*, 2010, pp. CMS5.

[49] S. Park, K. Kim, I. Kim and G. Kim, "Si micro-ring MUX/DeMUX WDM filters," *Optics Express*, vol. 19, pp. 13531-13539, 2011.

[50] M. A. Popovic, T. Barwicz, M. S. Dahlem, F. Gan, C. W. Holzwarth, P. T. Rakich, H. I. Smith, E. P. Ippen and F. X. Krtner, "Tunable, fourth-order silicon microring-resonator add-drop filters," in *33rd ECOC*, Germany, 2007, .

[51] Fengian Xia,Mike Rooks,Lidija Sekaric, and Yurii Vlasov, "ultra-compact high order ring resonator filters using submicron silicon photonic wires for on chip optical interconnections." *Optical Communications and Networking, IEEE/OSA Journal Of*, vol. 15, 2007.

[52] A. Melloni, "Synthesis of a parallel-coupled ring-resonator filter," *Opt. Lett.*, vol. 26, pp. 917-919, 2001.

[53] K. Ronse, "Optical lithography—a historical perspective," *Comptes Rendus Physique*, vol. 7, pp. 844-857, 2006.

[54] K. J. Vahala, "Optical microcavities," *Nature*, vol. 424, pp. 839-846, 2003.

[55] R. Mansoor, S. Koziel, H. Sasse and A. Duffy, "Crosstalk suppression bandwidth optimisation of a vertically coupled ring resonator add/drop filter," *IET Optoelectronics*, vol. 9, pp. 30-36, 2015.

[56] W. McKinnon, D. Xu, C. Storey, E. Post, A. Densmore, A. DelÔge, P. Waldron, J. Schmid and S. Janz, "Extracting coupling and loss coefficients from a ring resonator," *Optics Express*, vol. 17, pp. 18971-18982, 2009.

[57] O. S. Ahmed, M. A. Swillam, M. H. Bakr and Xun Li, "Efficient Design Optimization of Ring Resonator-Based Optical Filters," *Lightwave Technology, Journal Of*, vol. 29, pp. 2812-2817, 2011.

[58] O. Schwelb, "Transmission, group delay, and dispersion in single-ring optical resonators and add/drop filters-a tutorial overview," *Lightwave Technology, Journal Of*, vol. 22, pp. 1380-1394, 2004.

[59] (2013). *3D Electromagnetic Simulation software*. Available: www.cst.com.

[60] ITU Recommendation, "Spectral grids for WDM applications: DWDM frequency grid," vol. G.694, 2006.

[61] M. R. Jimenez, R. Passy, M. A. Grivet and J. P. von der Weid, "Computation of power penalties due to intraband crosstalk in optical systems," *Photonics Technology Letters, IEEE*, vol. 15, pp. 156-158, 2003.

[62] Eduward Tangdiongga, "Crosstalk Mitigation Techniques in Multi-Wavelength Networks Comprising Photonic Integrated Circuits," *PhD Thesis*, Eindhoven : Technische Universiteit, Netherlands, 2001.

[63] H. J. S. Dorren, H. de Waardt and I. T. Monroy, "Statistical analysis of crosstalk accumulation in WDM networks," *Lightwave Technology, Journal Of*, vol. 17, pp. 2425-2430, 1999.

[64] A. Chraplyvy, "Optical power limits in multi-channel wavelength-division-multiplexed systems due to stimulated Raman scattering," *Electron. Lett.*, vol. 20, pp. 58-59, 1984.

[65] T. Okoshi, *Coherent Optical Fiber Communications.* Boston, MA: Kluwer, 1988.

[66] A. Canciamilla, M. Torregiani, C. Ferrari, F. Morichetti, R. De La Rue, A. Samarelli, M. Sorel and A. Melloni, "Silicon coupled-ring resonator structures for slow light applications: potential, impairments and ultimate limits," *Journal of Optics*, vol. 12, pp. 104008, 2010.

[67] Y. Yanagase, S. Suzuki, Y. Kokubun and S. T. Chu, "Box-like filter response and expansion of FSR by a vertically triple coupled microring resonator filter," *Lightwave Technology, Journal Of*, vol. 20, pp. 1525-1529, 2002.

[68] J. Zhou, M. J. O'Mahony and S. D. Walker, "Analysis of optical crosstalk effects in multi-wavelength switched networks," *Photonics Technology Letters, IEEE*, vol. 6, pp. 302-305, 1994.

[69] H. Takahashi, K. Oda and H. Toba, "Impact of crosstalk in an arrayed-waveguide multiplexer on NxN optical interconnection," *Lightwave Technology, Journal Of*, vol. 14, pp. 1097-1105, 1996.

[70] H. W. Ott and H. W. Ott, *Noise Reduction Techniques in Electronic Systems.* Wiley, New York, 1988.

[71] M. Gustavsson, L. Gillner and C. P. Larsen, "Statistical analysis of interferometric crosstalk: theory and optical network examples," *Lightwave Technology, Journal Of*, vol. 15, pp. 2006-2019, 1997.

[72] P. André, J. Pinto, A. N. Pinto and T. Almeida, "Performance Degradations due to Crosstalk in Multiwavelength Optical Networks Using Optical Add Drop Multiplexers Based on Fibre Bragg Gratings," *Electrónica E Telecomunicações*, vol. 3, pp. 85-89, 2012.

[73] H. Simos, C. Mesaritakis, D. Alexandropoulos and D. Syvridis, "Intraband crosstalk properties of add–drop filters based on active microring resonators," *Photonics Technology Letters, IEEE*, vol. 19, pp. 1649-1651, 2007.

[74] O. Schwelb, "Crosstalk and bandwidth of lossy microring add/drop multiplexers," *Opt. Commun.*, vol. 265, pp. 175-179, 2006.

[75] T. Kato and Y. Kokubun, "Optimum coupling coefficients in second-order series-coupled ring resonator for nonblocking wavelength channel switch," *J. Lightwave Technol.*, vol. 24, pp. 991, 2006.

[76] Y. Goebuchi, T. Kato and Y. Kokubun, "Optimum arrangement of high-order series-coupled microring resonator for crosstalk reduction," *Japanese Journal of Applied Physics*, vol. 45, pp. 5769, 2006.

[77] C. J. Kaalund, "Critically coupled ring resonators for add-drop filtering," *Opt. Commun.*, vol. 237, pp. 357-362, 2004.

[78] X. Yang, M. Yu, D. Kwong and C. W. Wong, "All-optical analog to electromagnetically induced transparency in multiple coupled photonic crystal cavities," *Phys. Rev. Lett.*, vol. 102, pp. 173902, 2009.

[79] A. W. Poon, Xianshu Luo, Fang Xu and Hui Chen, "Cascaded Microresonator-Based Matrix Switch for Silicon On-Chip Optical Interconnection," *Proceedings of the IEEE*, vol. 97, pp. 1216-1238, 2009.

[80] N. Rouger, L. Chrostowski and R. Vafaei, "Temperature Effects on Silicon-on-Insulator (SOI) Racetrack Resonators: A Coupled Analytic and 2-D Finite Difference Approach," *Lightwave Technology, Journal Of*, vol. 28, pp. 1380-1391, 2010.

[81] R. D. Mansoor, H. Sasse, M. A. Asadi, S. J. Ison and A. Duffy, "Over Coupled Ring Resonator-Based Add/Drop Filters," *Quantum Electronics, IEEE Journal Of*, vol. 50, pp. 598-604, 2014.

[82] R. Mansoor, H. Sasse, S. Ison and A. Duffy, "Crosstalk bandwidth of grating-assisted ring resonator add/drop filter," *Opt. Quant. Electron.*, vol. 47, pp. 1127-1137, 2015.

Riyadh Dakhil Mansoor was born in Al Muthanna, Iraq, in 1975. He received the B.Eng. (Hons.) degree in electrical engineering and M.Sc. degree from the University of Basra, Basra, Iraq, in 1996 and 1998, respectively. He is currently pursuing the Ph.D. degree in optical communication with De Montfort University, Leicester, U.K.

Alistair P. Duffy was born in Ripon, U.K., in 1966. He received the B.Eng. (Hons.) degree in electrical and electronic engineering and the M.Eng. degree from University College, Cardiff, U.K., in 1988 and 1989, respectively, the Ph.D. degree from Nottingham University, Nottingham, U.K., in 1993, focusing on experimental validation of numerical modelling, and the M.B.A. degree from the Open University, Buckinghamshire, U.K., in 2003. He is currently a Professor in Electromagnetics with De Montfort University, Leicester, U.K. He has authored over 150 articles published in journals and presented at international symposia. His research interests include CEM validation, communications cabling, and technology management.